

1 Electronic supplementary information

2 **Ultra-fast and Robust Capture of Fluoride by Amino Terephthalic Acid Facilitated** 3 **Lanthanum Based Organic Framework: Insight into Performance and Mechanisms**

4

5 **Supporting Information**

6 **Batch experimental studies using La@ATPA and La@TPA**

7 The effect of initial pH on the uptake of fluoride by La@ATPA and La@TPA was studied over
8 pH 2-11. The initial concentration of fluoride was maintained at 5 mg/L with a sorbent dosage
9 of 1 g/L in a final volume of 20 mL. The suspensions were equilibrated for 2 h in an orbital
10 shaker at 110 rpm at 25°C. After equilibration, samples were filtered using 125 mm Whatmann
11 filter paper (11-micron pore size) and analysed for fluoride.

12 Sorption isotherm studies on La@ATPA and La@TPA were accomplished with batch
13 reactors containing varying initial concentrations of fluoride (5 mg/L to 1000 mg/L) with a
14 fixed sorbent dosage (1.0 g/L) in a total reactor volume of 20 mL at circumneutral pH. Reactors
15 were equilibrated for 2 h and analysed as before. The amount of F uptake by La@ATPA and
16 La@TPA and percentage F removal were evaluated using the following equations,
17 respectively:

$$18 \quad q_e = \frac{(C_0 - C_e)}{m} \times V \quad (1)$$

$$19 \quad \text{Removal percentage of fluoride (\%)} = \frac{(C_0 - C_e)}{C_0} \times 100 \quad (2)$$

20 where, q_e is the amount of fluoride sorbed (mg/g), C_0 and C_e are the initial and equilibrium
21 concentrations of fluoride (mg/L), m is the mass of sorbent (g), V is the total volume of the
22 reactor. Microsoft Excel 2019 has been used for the calculation of error bars. The expression
23 of the error functions is as follows ^{1,2} :

$$24 \quad \text{Average relative error (ARE)} = \frac{1}{N} \sum \frac{|Q_{cal} - Q_{exp}|}{Q_{exp}} \times 100 \quad (3)$$

25 Chi-square (X^2) = $\sum \frac{(Q_{exp} - Q_{cal})^2}{Q_{cal}}$ (4)

26 where N represents the experimental data points, $Q_{cal}(mg/g)$ and $Q_{exp}(mg/g)$ is the calculated
27 and experimental adsorption capacity of La@ATPA and La@TPA at equilibrium.

28 Kinetics of F sorption on both sorbents was quantified using a 10 mg/L fluoride solution
29 and an adsorbent dose of 1.0 g/L. The uptake of fluoride by various MOFs were monitored at
30 predefined time intervals. Potential interference of other anions and organic matter, like
31 chloride, nitrate, sulfate, bicarbonate, phosphate, arsenate and humic acid on F removal was
32 investigated by adding varying concentrations of interfering ions to 10 mg/L of F added to
33 ultrapure water. The concentrations of these ions tested were in accordance with their levels
34 typically present in groundwater. The solutions containing fluoride and interfering ions were
35 equilibrated with 1 g/L of La@ATPA for 2 h, filtered and analysed for fluoride.

36 To study the recyclability of the sorbent, F desorption studies were carried out after
37 fluoride was loaded on La@ATPA. Fluoride-loaded La@ATPA was contacted with 20 mL of
38 varying concentrations of alkali (0.01, 0.1, 0.5, 1.0 M). The suspensions were equilibrated for
39 2 h in an orbital shaker maintained at 110 rpm. After equilibration, suspensions were filtered
40 and analysed for F. The desorbed sorbent was washed with water to remove the alkalinity and
41 the cycles were repeated.

42 Leaching studies were conducted on fluoride-loaded La@ATPA. Initially, 0.05 g of
43 La@ATPA was equilibrated with a solution containing 10 mg/L of F. After sorption, the
44 suspensions were filtered and F-loaded sorbent were equilibrated with different pH (3.0, 3.6,
45 4.1, 5.35 and 6.3) for 24 h, after which samples were drawn, filtered, and analyzed for fluoride.
46 To further assess the long-term leachability of fluoride, around 0.05 g of F-loaded La@ATPA
47 was equilibrated in both 100 mL each of DI water and groundwater for a period of one week.
48 The application of La@ATPA on real fluoride-contaminated groundwater samples was also
49 evaluated. The samples were collected from three locations of Bansathi village, Kanpur Nagar

50 and Uttar Pradesh. Most of the groundwater sources in that village were contaminated by
51 fluoride (Supporting Information Table S1).³ The three locations were chosen based on
52 different levels of fluoride concentrations (2.0, 4.8, 6.0 mg/L) in the handpumps. Samples were
53 collected in 1 L Tarson HDPE wide-mouthed bottles. The bottles were cleaned thoroughly with
54 ultrapure water prior to sampling. Before sample collection, ~20 L of stagnant water were
55 discarded from each handpump. The bottles were capped tightly and wrapped with Parafilm to
56 ensure that no atmospheric exchange occurs during transportation to the laboratory.
57 Additionally, two samples of IIT Kanpur groundwater with an inherent F concentration of
58 0.982 mg/L, spiked with 4 mg/L and 8 mg/L of fluoride, were also tested. For each experiment,
59 20 mL of the samples were equilibrated with La@ATPA at a dosage of 2.5 g/L for 2 h. The
60 equilibrated suspensions were filtered and the supernatants were analyzed for fluoride. All
61 batch experiments described above were conducted in triplicate and the average of the three
62 readings were recorded.

63 **Characterization studies and analysis of aqueous and solid samples**

64 Fluoride was determined by a Thermo Orion meter using a fluoride ion-selective electrode.
65 The meter was first calibrated with standard solutions of 0.5, 5 and 10 mg/L of fluoride. For
66 each analysis, the total ionic strength adjustment buffer (TISAB) was mixed with standards
67 and samples in a ratio of 1:1 to prevent the formation of metal-fluoride complexes. A pH meter
68 (pH510 Eutech) was used to analyse the pH of the solution. Analysis of phosphate (PO_4^{3-}),
69 sulphate (SO_4^{2-}), nitrate (NO_3^-) and chloride (Cl^-) were carried out using Metrohm 882 compact
70 ion chromatography (IC). 1 mM sodium bicarbonate in 3.2 mM sodium carbonate buffer was
71 used as eluent using Metrosep A Supp 5 column. The flow rate of the eluent was maintained at
72 0.7 mL/min. The lower limit of detection was found to be 0.1 mg/L for IC. Inductively coupled
73 plasma-mass spectrometry (ICP-MS; Thermo Scientific X-SERIES 2) was used to analyse
74 arsenic (As), cadmium (Cd), chromium (Cr), and copper (Cu). The lower limit of detection for

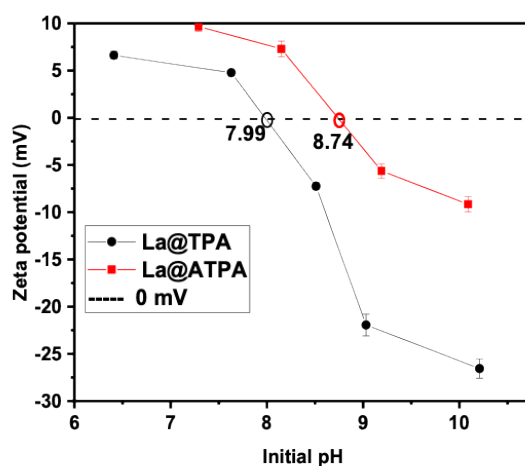
75 the method was 2 ng/L. Total dissolved solids were measured by a TDS meter (HACH,
76 HQ30d). Alkalinity was determined by titration using 0.02 N standard sulphuric acid as titrant
77 and methyl orange solution as indicator. Hardness was analyzed by titrimetry using
78 ethylenediaminetetraacetic acid as a reagent and Eriochrome Black T as an indicator.
79 Point of zero charge values of La@TPA and La@ATPA were measured using Brookhaven
80 ZetaPALS connected to BI-ZTU auto-titrator. Samples were prepared by dispersing 0.6 g of
81 material in 80 mL of 0.01 M KNO₃.⁴ The suspensions were stirred using a magnetic stirrer at
82 110 rpm for 24 h to achieve equilibration. Prior to measurements, the solutions were sonicated
83 for 10 min and kept undisturbed for 1 h for settling after which supernatants were collected for
84 analysis.

85 The morphology of synthesised MOF La@ATPA was analyzed using field emission
86 scanning electron microscopy (FE-SEM; FEI Quanta 200) at macroscopic scale and by
87 transmission electronic microscopy (TEM; Technai G2 T-20 FEI) at a higher resolution. For
88 TEM analysis samples were ultrasonicated with ethanol for 15 min at room temperature. Then,
89 ethanol dispersed sample droplets were placed on the copper grid (3mm diameter) and vacuum
90 dried. The infrared spectrum of MOF was analysed in attenuated total reflectance (ATR) mode
91 by Fourier-transform infrared spectrometry (FTIR; Bruker) with KBR pellets. The prevalent
92 phases in the sorbents were studied using an X-ray diffractometer (XRD; Hecus S3 micro). The
93 sample angle (2θ), from 5 to 80 °C was measured at 45 kV and 40 mA. The oxidation states
94 and chemical composition of La@ATPA were analysed using X-ray photoelectron
95 spectroscopy (XPS; PHI 5000 Versa Probe II) with a monochromatic Mg K α . Deconvolution
96 of individual molecular orbital peaks of various elements was carried out using XPSPEAK41
97 software.⁵ The BET surface area and pore volume were analysed by the Autosorb 1-C
98 instrument (AS1-C, Quantachrome). The N₂ adsorption desorption curve has been plotted as
99 reported by Zhang et al.^{4,5}

100 Geochemical analysis

101 Dissolved solute data were analyzed for chemical equilibrium speciation with well-known
102 modelling software, Visual MINTEQ 3.1.⁶ All ionic strength corrections were performed using
103 the Davies equation. Solubility (log C-pH) plots were prepared by considering the infinite mass
104 of the relevant solid, LaF₃(s). The default database of Visual MINTEQ 3.1 was used for all the
105 thermodynamic analyses. All calculations were performed considering the system as closed to
106 the atmosphere.

107



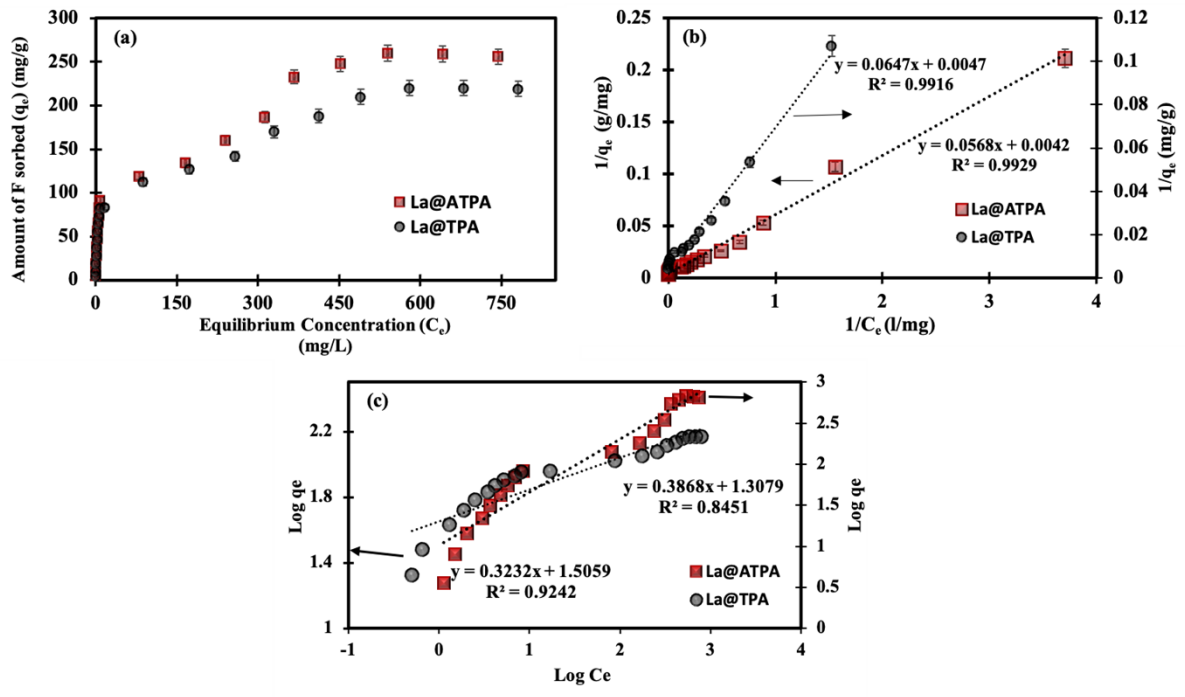
108

109 **Figure S1. Zeta potential of the two sorbents (La@TPA and La@ATPA) was used for the**
110 **F sorption study.**

111

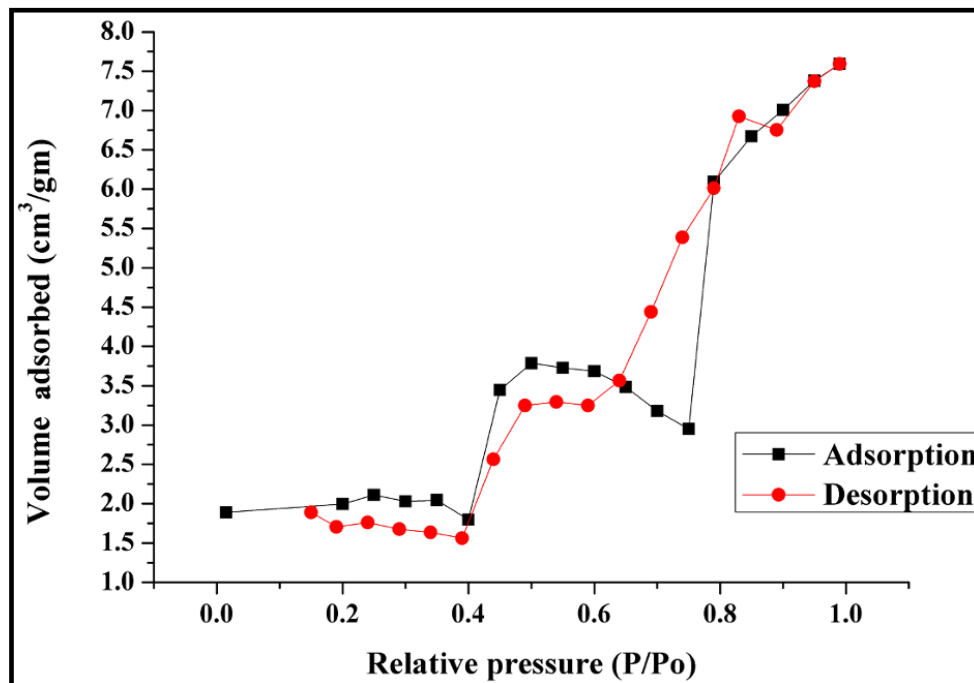
112

113



114
 115
 116
 117
 118
 119

Figure S2. Fluoride uptake on La@TPA and La@ATPA sorbents: (a) Equilibrium sorption isotherm, (b) Linearized Langmuir plot and (c) Linearized Freundlich plot.



120
 121
 122
 123

Figure S3. N₂ adsorption-desorption curves of La@ATPA

124

125

126

Table S1. Details of real contaminated groundwater sampling locations.

Sample ID	Latitude (N)	Longitude (E)	Depth (m)
S1	26° 34' 28.4412"	80° 9' 13.3704"	12
S2	26° 34' 29.1036"	80° 9' 11.754"	11
S3	26° 34' 31.8828"	80° 9' 11.9376"	12

127

128

129

130

131

132

133

Table S2. Specific surface area and pore volumes of La@ATPA

Parameter	Values
Specific Surface Area (m ² /g)	18.14
Average Pore Diameter (nm)	5.91
Total Pore Volume (cc/g)	0.0268
Micropores (%)	2.0
Mesopores (%)	84.2
Macropores (%)	13.8



139

140 **Table S3. Comparison of adsorption capacities of various MOFs towards defluoridation**

S.No	MOF	pH	Langmuir Adsorption Capacity (mg/g)	Equilibrium Time (mins/hrs.)	Ref.
1	Sn (II)-TMA MOF	3-10	30.86	150 mins	7
2	MOF-801	-	19.42	120 mins	8
3	Ce-BDC-48	-	128.0	85 mins	9
4	MIL-96(Al)	3	42.9	90 mins	10
5	UiO-66-amine	7	41.5	-	11
6	MIL-96	7	21.2	-	12
7	Aluminum Fumarate	7	600.0	24 hrs	13
8	Al. Fumarate and PAN	7	205.0	6 hrs	14
9	Ce-MIL-96	3-10	38.65	-	15
10	Al Fumarate + Cellulose acetate	7	179.0	-	16
11	Zr-MOF	-	102.4	20 mins	17
12	Ce-BPDC	6	45.5	20 mins	18
13	La@ABDC	3-9	4.95	30 mins	19
14	UiO-66-NH2 CNM	4-10	95	60 mins	20
15	Ce@ABDC and Ce@BDC	6-7	4.91 and 4.88	30 mins	21
16	La-BTC, La-BPDC, La-BHTA, La-PMA, and La-BDC	4-9	105.2, 125.9, 145.5, 158.9, and 171.7	180 mins	22
17	NH ₂ -MIL-53(Al)	7	202.5	-	23
18	R-MIL-100(Fe)	6.5	23.53	1.5 hrs	24
19	La-BTC	3	155.92	-	25
20	La@TPA La@ATPA	4-8 3-10	212.7 232.5	3 hrs 90 mins	Present Work

141
142
143
144
145
146
147
148

Table S4. XPS Analysis of La@ATPA before and after fluoride loading

Sample	Element	Binding Energy (eV)		Inference
La@ATPA	La 3d5/2	833.6 836.3		La-O bond
F-La@ATPA	La 3d5/2	833.7 835.9 832.0 834.6		La-O bond La-F bond
F-La@ATPA	F1s	681.9 682.5 683.2 684.7		OH ₃ ⁺ ---F -NH ₃ ⁺ ---F physisorbed fluoride La-F
La@ATPA	N1s	397.4 403.7		Amino group Nitro group
F-La@ATPA	N1s	397.2 403.5 398.1		Amino group Nitro group -NH ₃ ⁺ ---F

150
151
152
153
154
155
156
157
158
159
160
161
162
163
164
165
166
167
168
169
170
171
172
173
174
175
176
177
178

179

180 **References**

181

- 182 1. B.A. Ezeonuegbu, D.A Machido, C.M. Whong, W.S. Japhet ,A. Alexiou , S.T.Elazab
183 ,N. Qusty, C.A. Yaro, G.E. Batiha, Agricultural waste of sugarcane bagasse as an
184 efficient adsorbent for lead and nickel removal from untreated wastewater: Biosorption,
185 equilibrium isotherms, kinetics and desorption studies. *Biotechnol. Rep.*,2021, 30,
186 e00614.
- 187 2. D. Gomez, C. Rodrigues, F.R. Lapolli, and M.A. Lobo-Recio, Adsorption of heavy
188 metals from coal acid mine drainage by shrimp shell waste: Isotherm and continuous-
189 flow studies. *J. Environ. Chem. Eng.*, 2019, 7(1), 102787.
- 190 3. A. K. Mohapatra, S. Sujathan, A. S. Ekamparam and A. Singh, The role of
191 manganese carbonate precipitation in controlling fluoride and uranium mobilization in
192 groundwater, *ACS Earth Space Chem.*, 2021, 5(10), 2700-2714.
- 193 4. O. S. Pokrovsky and J. Schott, Surface chemistry and dissolution kinetics of divalent
194 metal carbonates, *Environ. Sci. Technol.*, 2002, 36(3), 426-432.
- 195 5. R. Kwok, 2000, XPS Peak Fitting Program for WIN95/98 XPSPEAK Ver.
196 4.1. <http://www.phy.cuhk.edu.hk/~surface/XPSPEAK/>.
- 197 6. J.P. Gustafsson, 2017 Visual MINTEQ, V 3.1, Department of Land and Water
198 Resources Engineering, KTH, Stockholm, Sweden.
- 199 7. A. Ghosh and G. Das, Green synthesis of a novel water-stable Sn (ii)-TMA metal–
200 organic framework (MOF): an efficient adsorbent for fluoride in aqueous medium in a
201 wide pH range, *New J. Chem.*, 2020, 44(4), 1354-1361.
- 202 8. T. L. Tan, H. Nakajima and S.A. Rashid, Adsorptive, kinetics and regeneration studies
203 of fluoride removal from water using zirconium-based metal organic frameworks, *RSC*
204 *Adv.*, 2020, 10(32), 18740-18752.

- 205 9. J. He, Y. Xu, Z. Xiong, B. Lai, Y. Sun, , Y. Yang and L. Yang, The enhanced removal
206 of phosphate by structural defects and competitive fluoride adsorption on cerium-based
207 adsorbent, *Chemosphere.*, 2020, **256**, 127056.
- 208 10. X. Wang, , H. Zhu, T. Sun, Y. Liu, T. Han, J. Lu and L. Zhai, Synthesis and Study
209 of an Efficient Metal-Organic Framework Adsorbent (MIL-96 (Al)) for Fluoride
210 Removal from Water, *J. Nanomater.*, 2019, **2019**.
- 211 11. M. Massoudinejad, M. Ghaderpoori, A. Shahsavani and M.M. Amini, Adsorption of
212 fluoride over a metal organic framework Uio-66 functionalized with amine groups and
213 optimization with response surface methodology, *J. Mol. Liq.*, 2016, **221**, 279-286.
- 214 12. N. Zhang, X. Yang, X. Yu, Y. Jia, J. Wang, L. Kong and J. Liu, Al-1, 3, 5-
215 benzenetricarboxylic metal-organic frameworks: A promising adsorbent for
216 defluoridation of water with pH insensitivity and low aluminum residual, *Chem. Eng.*
217 *J.*, 2014, **252**, 220-229.
- 218 13. J. Dechnik, C. Janiak and S. De, Aluminium fumarate metal-organic framework: a
219 super adsorbent for fluoride from water, *J. Hazard. Mater.*, 2016, **303**, 10-20.
- 220 14. S. Karmakar, S. Bhattacharjee and S. De, Aluminium fumarate metal organic
221 framework incorporated polyacrylonitrile hollow fiber membranes: spinning,
222 characterization and application in fluoride removal from groundwater, *Chem. Eng. J.*,
223 2018,**334**, 41-53
- 224 15. X. Yang, S. Deng, F. Peng and T. Luo, A new adsorbent of a Ce ion-implanted metal-
225 organic framework (MIL-96) with high-efficiency Ce utilization for removing fluoride
226 from water, *Dalton Trans.*, 2017, **46**(6), 1996-2006.
- 227 16. S. Karmakar, S. Bhattacharjee and S. De, Experimental and modeling of fluoride
228 removal using aluminum fumarate (AlFu) metal organic framework incorporated

- 229 cellulose acetate phthalate mixed matrix membrane, *Environ. Sci. Water Res. Technol.*,
230 2017, **5**(6), 6087-6097.
- 231 17. J. He, X. Cai, K. Chen, Y. Li, K. Zhang, Z. Jin and J. Liu, Performance of a novel-
232 defined zirconium metal-organic frameworks adsorption membrane in fluoride
233 removal, *J. Colloid Interface Sci.*, 2016, **484**, 162-172.
- 234 18. C. Zhao, Y. Cui, F. Fang, S. O . Ryu and J. Huang, Synthesis of a novel Ce-bpdc for
235 the effective removal of fluoride from aqueous solution, *Adv. Condens. Matter Phys.*,
236 2017.
- 237 19. A. Jeyaseelan and N. Viswanathan, Design of amino-functionalized benzene-1, 4-
238 dicarboxylic acid-fabricated lanthanum-based metal–organic frameworks for
239 defluoridation of water. *J. Chem. Eng. Data* ., 2020, **65**(11), 5328-5340.
- 240 20. A. Mohamed, E. P. V. Sanchez, E. Bogdanova, B. Bergfeldt, A. Mahmood, , R. V.
241 Ostvald, and T. Hashem, Efficient fluoride removal from aqueous solution using
242 zirconium-based composite nanofiber membranes. *Membranes.*, 2021, **11**(2), 147.
- 243 21. A. Jeyaseelan, M. Naushad, T. Ahamad and N. Viswanathan, Fabrication of amino
244 functionalized benzene-1, 4-dicarboxylic acid facilitated cerium based metal organic
245 frameworks for efficient removal of fluoride from water environment, *Environ. Sci.*
246 *Water Res. Technol.*, 2021, **7**(2), 384-395.
- 247 22. C. Yin, Q. Huang, G. Zhu, L. Liu, S. Li, X. Yang and S. Wang, High-performance
248 lanthanum-based metal–organic framework with ligand tuning of the microstructures
249 for removal of fluoride from water, *J. Colloid Interface Sci.*, 2022, **607**, 1762-1775.
- 250 23. D. H. Xie, , X. Ge, W. X. Qin and Y. X. Zhang, NH₂-MIL-53 (Al) for simultaneous
251 removal and detection of fluoride anions, *Chinese J. Chem. Phys.*, 2021, **34**(2), 227-
252 237.

- 253 24. W .Li, T .Zhang, L. Lv, Y. Chen, W. Tang and S. Tang, Room-temperature synthesis
254 of MIL-100 (Fe) and its adsorption performance for fluoride removal from water,
255 *Colloids Surf. A Physicochem. Eng. Asp.*, 2021, **624** , 126791.
- 256 25. Yang, Y., Li, X., Gu, Y., Lin, H., Jie, B., Zhang, Q., & Zhang, X. (2022). Adsorption
257 property of fluoride in water by metal organic framework: optimization of the process
258 by response surface methodology technique. *Surfaces and Interfaces*, 28, 101649.
- 259
- 260
- 261
- 262
- 263
- 264
- 265